Showa Univ J Med Sci **24**(2), 77～87, June 2012

Original

A Study of Correlation between Gd-EOB-DTPA-enhanced MRI Using the 3T MRI System and Tc-99m-GSA Hepatic Scintigraphy / Hepatic Function Tests in Prehepatectomy Cases

Jumpei SUYAMA[1], Akira SHINOZUKA[1], Yoshimitsu OHGIYA[1], Takehiko GOKAN[1], Toshiyuki BABA[2], Michio IMAWARI[2], Takeshi AOKI[3] and Masahiko MURAKAMI[3]

Abstract: This study compared results from Gd-EOB-DTPA on two different phases of 3T MRI with those from Tc-99m-GSA hepatic scintigraphy and hepatic function tests. Twenty-four patients with liver tumor were included in this study. All patients underwent Gd-EOB-DTPA-enhanced-MRI and Tc-99m-GSA hepatic scintigraphy. Clearance index (HH15) and receptor index (LHL15) were calculated for the Tc-99m-GSA, while signal intensities (SI) of liver at pre-injection and at 4 / 20 min post-injection, and of spleen at 4 min / 20 min were measured (SI_{pre}, SI_{4min}, SI_{20min}, SI_{sp4min}, $SI_{sp20min}$, respectively) for the Gd-EOB-DTPA-MRI. Liver activity at 15 min by Tc-99m-GSA scintigraphy or biochemical liver function values were compared with liver spleen contrast at 4 min ($LSC_{4min} = SI_{4min} / SI_{sp4min}$) or 20 min post-injection ($LSC_{20min} = SI_{4min} / SI_{SP20min}$), and the increase in ratio at 4 min ($IR_{4min} = SI_{4min} / SI_{sp4min}$) or 20 min ($IR_{20min} = SI_{20min} / SI_{pre}$). Total bilirubin levels (T-bil), serum albumin levels (Alb), prothrombin activity, and the indocyanine green clearance test (ICG) results were also analyzed. There were statistically significant correlations in all comparisons between Gd-EOB-DTPA and Tc-99m-GSA. The highest coefficient of correlation was obtained in IR_{4min} (LHL15 : $r = 0.795$, $P < 0.001$; HH15 : $r = -0.782$, $P < 0.001$), with IR_{20min} (LHL15 : $r = 0.690$, $P < 0.01$; HH15 : $r = -0.528$, $P < 0.05$), LSC_{4min} (LHL15 : $r = 0.458$, $P < 0.05$; HH15 : $r = -0.626$, $P < 0.05$), and LSC_{20min} (LHL15 : $r = 0.443$, $P < 0.05$, HH15 : $r = -0.609$, $P < 0.05$) also significantly correlated. Correlations in hepatic function data were observed between IR_{4min} and T-bil / Alb, and IR_{20min} and Alb. In 3T-MRI using Gd-EOB-DTPA, the SI of liver at pre- to post-injection (especially at 4 min) significantly correlated with the corresponding Tc-99m-DTPA scintigraphy results, and with some biochemical liver function data.

Key words: MRI, gadolinium ethoxybenzyl diethylenetriaminepentaacetic acid (Gd-EOB-DTPA), technetium-99m-galactosyl human serum albumin (Tc-99m-GSA), liver function

[1] *Department of Radiology, Showa University School of Medicine*, 1-5-8 Hatanodai, Shinagawa-ku, Tokyo 142-8666, Japan.
[2] *Department of Internal Medicine, Division of Gastroenterology, Showa University School of Medicine.*
[3] *Department of Surgery, Division of General and Gastroenterological Surgery, Showa University School of Medicine.*

Introduction

Gadolinium ethoxybenzyl diethylenetriaminepentaacetic acid (Gd-EOB-DTPA) has been widely used as a magnetic resonance imaging (MRI) contrast medium for the diagnosis of liver tumors, including hepatoma, and its usefulness for evaluating hepatic function has been demonstrated by a number of studies[1–4]. Approximately 40% of Gd-EOB-DTPA administered to the body is excreted in bile and thus its use in the evaluation of hepatic function has been considered since the development of this approach. The Child-Pugh classification and the uptake of ethoxybenzyl (EOB) in the liver were thus also used to confirm the reduction in signal enhancing effect in the hepatic parenchyma of patients with severe hepatic dysfunction[1–5].

Technetium-99m-galactosyl human serum albumin (Tc-99m-GSA) has also been used in the clinical setting to visually assess hepatocellular function since the first half of 1990. This medium is taken up by hepatocytes via asialoglycoprotein receptors on the hepatic membrane and is excreted in bile. There are various analytical methods for the evaluation of hepatic function using Tc-99m-GSA, with the most widely used being the clearance index (HH15) and the receptor index (LHL15). These indicators are easy to use and show good correlation with hepatic reserve[6, 7]; they have also been used recently in postoperative follow-up for hepatectomy, preoperative volumetry assessment of liver remnant functions[8, 9], and evaluation of hepatic functions after living donor liver transplantation[9, 10].

Both Gd-EOB-DTPA and Tc-99m-GSA are taken up by hepatocytes and excreted in bile, and it is therefore reasonable to assume that both could be used to evaluate hepatic function. Indeed, previous comparisons of liver spleen contrast (LSC)[1] as well as bile duct signal[11] and hepatic functions have demonstrated correlations between Gd-EOB-DTPA and hepatic function. Here we tested this assumption by comparing the increase ratio (IR) of the liver signal / LSC when MRI was performed using Gd-EOB-DTPA with HH15 and LHL15 obtained using Tc-99m-GSA and hepatic function testing. It should be noted that a similar previous study focused on the hepatobiliary phase[1, 2]; however, the excretion to bile from hepatocytes differs between EOB and GSA. We therefore assessed Gd-EOB-DTPA-enhanced MRI both at the phase less influenced by the excretion to bile and the hepatobiliary phase.

Subjects and Methods

The subjects included 24 patients (16 males and 8 females) who underwent both preoperative Gd-EOB-DTPA-enhanced MRI using the 3-Tesla MRI system and Tc-99m-GSA hepatic scintigraphy within 1 month of admission to hospital from July 2008 to October 2009 (interval range 1～30 days; mean interval 12.8 days). Subject age ranged from 31 to 78 years with a mean age of 66.0 years. The patients' diseases included hepatocellular carcinoma (n＝14), cholangiocellular carcinoma (n＝5), and hepatic metastases (n＝5).

According to the Child-Pugh classification, 22 patients were classified as Class A, 2 as Class B, and none as Class C. The primary disease of both patients classified as Class B was hepatocellular carcinoma.

Magnetic Resonance Imaging (MRI)

MRI was performed using the MAGNETOME Trio A Tim System 3.0T (Siemens Medical Solutions, Erlangen, Germany), with either a body-matrix-coil or spine-matrix-coil 4ch. The imaging sequence was VIBE with fat suppression (CHESS) (TR, 3.29 ms ; TE, 1.22 ms ; flip angle, 13° ; FOV, 350 mm ; Matrix, 216×320 ; 56 slices ; slice thickness, 3.5 mm ; acquisition time, 21 s). The patients were instructed to fast for at least three hours or more before the test. Gd-EOB-DTPA (0.025 mmol / kg body weight) was intravenously infused at 2 ml / s, and subsequently flushed out with 20 ml of physiological saline. Images were taken before, and at 4 and 20 min after injection of the contrast material.

The signal intensity (SI) of the liver was measured in a region of interest (ROI) of approximately 150 mm^2 in the medial and lateral segments of the left lobe, and in the anterior and posterior segments of the right lobe. The average of these values was determined as the signal intensity of the liver (SI_L). The spleen SI was measured in two ROIs, at the anterior and posterior segments of the spleen in the same slice as that used above, and the average was determined as SI_S. SI_L and SI_S were measured before injection, and at 4 and 20 min after contrast material injection. Increase ratio (IR) and liver spleen contrast (LSC) before imaging relative to those 4 and 20 min after contrast material injection were calculated using the following formulae :

$IR_{4min} = SI_{L4min} / SI_{LPRE}$,

$IR_{20min} = SI_{L20min} / SI_{LPRE}$,

$LSC_{4min} = SI_{L4min} / SI_{S4min}$,

$LSC_{20min} = SI_{L20min} / SI_{S20min}$.

SIs of the common hepatic duct and common bile duct were measured and the mean SI was calculated (SIb), as was the mean SI of the right erector spinae muscle (SIm). Relative SI was calculated as follows :

Relative SI = SIb / SIm.

^{99m}Tc-GSA scintigraphy

The patients were instructed to fast for three hours or more before testing, and then were intravenously infused with 185 MBq of 99mTc-GSA, which was flushed out with 40 ml of physiological saline. Images were taken using a PRISM 2000XP scintillation camera [Philips (Picker)] with a dual-head system and a low-energy high-resolution collimator. A frontal view was taken in the supine position. Serial scans were acquired with the collection matrix of 128×128, 15 s / frame×80 frames (20 min). Image processing [Odyssey : Philips (Picker)], was used to select the ROIs over the heart and liver for each time activity curve, which

were used to obtain the counts for the heart and liver at 3 and 15 min after the intravenous infusion. HH15 and LHL15 were calculated using the following formulae:

HH15 = (heart count at 15 min) / (heart count at 3 min)

LHL15 = (liver count at 15 min) / (sum of liver and heart counts at 15 min)

Statistical Analysis

The correlation coefficients between IR_{4min}, IR_{20min}, LSC_{4min}, LSC_{20min}, HH15, and LHL15, and the biochemical test data including total bilirubin (T-bil), albumin (Alb), prothrombin time (PT), ICG_{R15} (n = 19), and estimated glomerular filtration rate (eGFR) were obtained. Significance levels were set at $P < 0.05$.

Results

The correlations among the IR of the liver signal at 4 min (IR_{4min}) and 20 min (IR_{20min}) after the infusion, the LSC at 4 min (LSC_{4min}) and 20 min (LSC_{20min}) after the infusion, and HH15 and LHL15 are shown in Fig. 1(a)-(d) and Table 1. Significant correlations were found between HH15 / LHL15 and both liver IR and LSC. The highest correlation coefficient was observed between IR_{4min} and LHL15, while the correlations of LHL15 with LSC_{4min} and LSC_{20min} were lower than those measured among the other parameters. The correlation coefficient of HH15 / LHL15 with the liver IR was greater for IR_{4min} than for IR_{20min}.

Correlations with hepatic function examination data were observed between IR_{4min} and T-bil / Alb, and between IR_{20min} and Alb, but there were no correlations for LSC_{4min} and LSC_{20min} (Table 2).

From the changes over time in liver SI after the infusion, the intensity 20 min after the infusion increased in 21 subjects (87.5%) and decreased in 3 subjects (12.5%), compared with 4 min after the infusion (Fig. 2). The latter subjects were all classified as Class A according to the Child-Pugh classification.

In this study, no visualization of contrast media inflow to the bile ducts was observed at 4 min after the infusion, while the bile ducts were visible in all cases at 20 min after the infusion. There were no differences in bile duct SIs between the groups with lowered and increased SI in the hepatic parenchyma 20 min after the infusion. The mean relative SI, excluding signal decreases at 20 min, was 4.70 ± 1.79. In the signal-decreased group, only one patient showed a higher than average SI (relative SI 7.62); for the other two patients, SI was below the average value (relative SI 2.38 and 2.62, respectively).

In three patients, Gd-EOB-DTPA did not reach the bile duct completely, thus these cases were excluded from the signal-decreased group. The primary diseases of these cases was hepatocellular carcinoma in one patient, hepatic metastases in one patient, and cholangiocellular carcinoma in one patient, and the size was 2.8 cm, 1.8 cm, and 1.2 cm in diameter, respectively. The hepatocellular carcinoma and hepatic metastases both developed in the

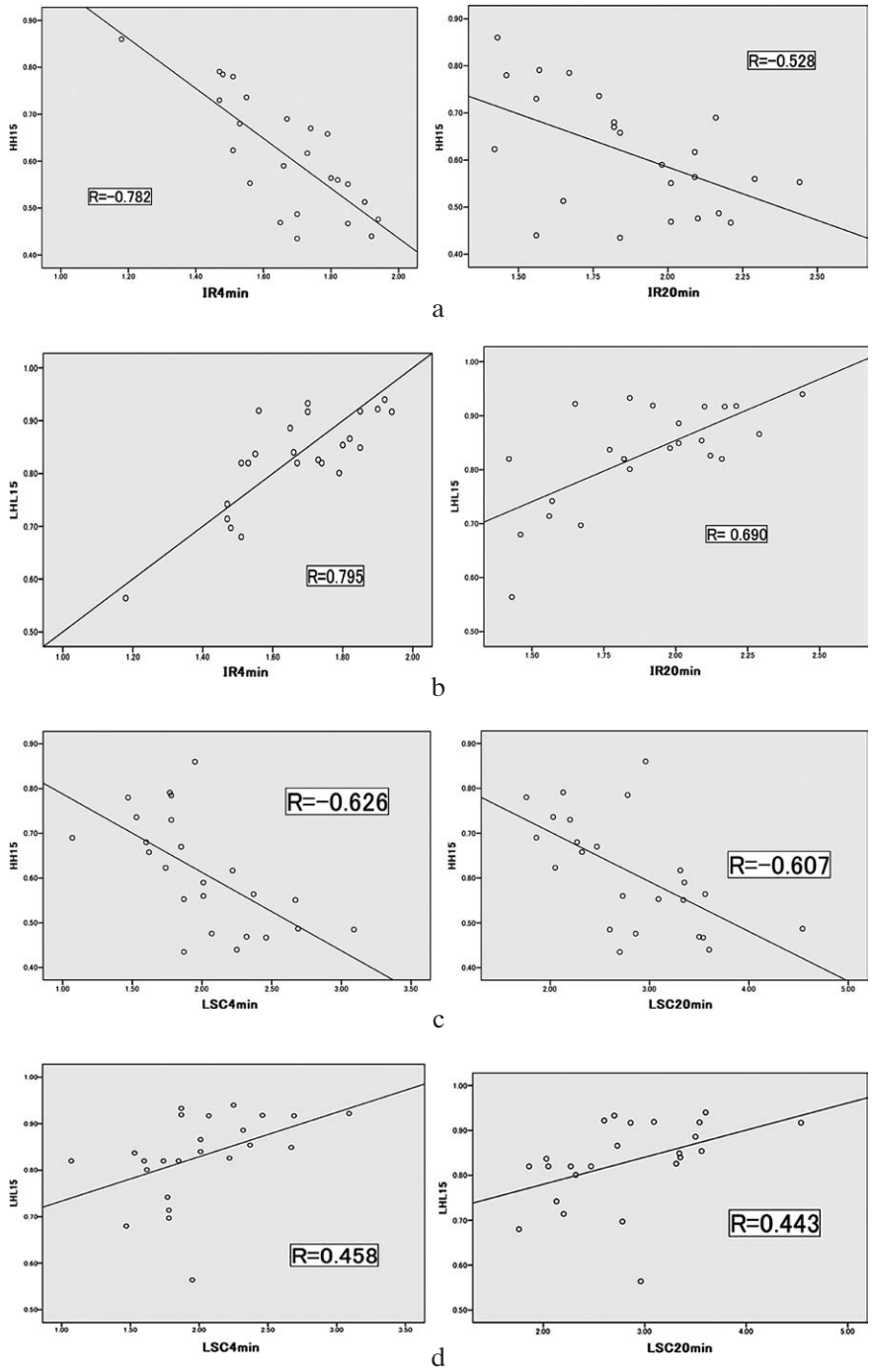

Fig. 1. Scatter plot showing the relationship between Tc-99m-GSA and Gd-EOB-DTPA
A statistically significant correlation was observed in all combinations.
a : HH15 and increase ratio at 4 min (IR_{4min}, IR_{20min})
b : LHL15 and increase ratio (IR_{4min}, IR_{20min}).
c : HH15 and liver spleen contrast (LSC_{4min}, LSC_{20min}).
d : LHL15 and liver spleen contrast (LSC_{4min}, LSC_{20min}).

Table 1. Correlations between data from Gd-EOB-DTPA and Tc-99m-GSA, indicating a statistically significant correlation for all combinations

	LHL15	HH15
IR4	R = 0.795 ($P < 0.001$)	R = −0.782 ($P < 0.001$)
IR20	R = 0.690 ($P < 0.01$)	R = −0.528 ($P < 0.01$)
LSC4	R = 0.458 ($P < 0.05$)	R = −0.626 ($P < 0.01$)
LSC20	R = 0.433 ($P < 0.05$)	R = −0.607 ($P < 0.01$)

Table 2. Correlations between measurements and indicators of hepatic function / GFR (n = 24 ; ICG15 only n = 19)

	T-bil	Alb	ICG15	PT	GFR
LHL15	0.725 ($P < 0.001$)	0.456 ($P < 0.05$)	0.426 (n.s.)	0.313 (n.s.)	0.345 (n.s.)
HH15	0.666 ($P < 0.01$)	0.406 ($P < 0.05$)	0.487 ($P < 0.05$)	0.267 (n.s.)	0.260 (n.s.)
IR_{4min}	0.532 ($P < 0.05$)	0.441 ($P < 0.05$)	0.325 (n.s.)	0.286 (n.s.)	0.243 (n.s.)
IR_{20min}	0.224 (n.s.)	0.421 ($P < 0.05$)	0.141 (n.s.)	0.324 (n.s.)	0.070 (n.s.)
LSC_{4min}	0.325 (n.s.)	0.398 (n.s.)	0.371 (n.s.)	0.062 (n.s.)	0.057 (n.s.)
LSC_{20min}	0.392 (n.s.)	0.323 (n.s.)	0.422 (n.s.)	0.063 (n.s.)	0.131 (n.s.)

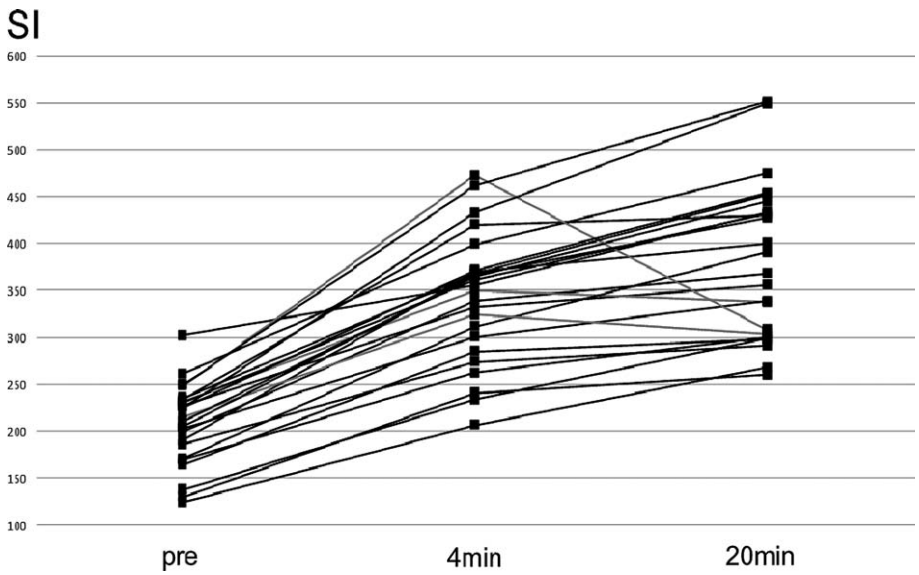

Fig. 2. Changes in liver signal intensity over time
In three cases the signal intensity decreased from 4 minutes to 20 minutes.

margin of the liver and there were no findings suggesting intrahepatic biliary stenosis. On the other hand, the patient with cholangiocellular carcinoma had stenosis in the intrahepatic bile duct of the left lobe, and contrast media inflow was visualized in the intrahepatic bile duct of the right lobe and in part of the bile duct, but not in the intrahepatic bile duct of the left lobe. IR_{4min} of these 3 patients ranged from 1.56 to 1.85, the SI gradually increased up to 20 min after the infusion, and Gd-EOB-MRI revealed no distinct findings. The Child-Pugh classification of these cases was Class A. In addition, the ICG test result was slightly high in the patient with hepatocellular carcinoma and the patient with hepatic metastases (11% and 16%, respectively), while it was normal in the patient with cholangiocellular carcinoma (4%).

When all patients in this study were divided according to the primary disease into the hepatocellular carcinoma group (n = 14) and non-hepatocellular carcinoma group (n = 10), the correlations between IR_{4min} and LHL15 were significantly different at R = 0.766 ($P < 0.01$) and R = 0.690 ($P < 0.05$), respectively. Dividing the non-hepatocellular carcinoma group further into the hepatic metastases group (n = 5) and cholangiocellular carcinoma group (n = 5) produced no significant differences in the same correlation (R = 0.800 and R = 0.719, respectively).

Discussion

In this study, the IR in the hepatic parenchyma before the EOB infusion, and at 4 and 20 min after the EOB infusion, and the LSC at 4 and 20 min after the infusion were used as evaluation parameters of Gd-EOB-DTPA for correlative comparison with HH15 and LHL15 of Tc-99m-GSA and various hepatic function evaluation data. The IR in the hepatic parenchyma and the LSC correlated positively with HH15 and LH15, with the coefficients of correlation in both cases higher at 4 min after the infusion than at 20 min after the infusion. In addition, hepatic function indicators, T-bil and Alb, correlated strongly with the IR in the hepatic parenchyma, but not with LSC.

Among previous studies that evaluated hepatic function using Gd-EOB-DTPA, Motosugi *et al*[1] showed a correlation between the LSC and hepatic function, while Takao *et al*[11] reported that the relative SI ratios of skeletal muscles to the right and left hepatic ducts, common hepatic duct, and common bile duct delayed the rate of SI increase in patients with chronic liver disease, that the rate of SI increase was slower in the chronic liver disease group than in the normal group, and that SI significantly correlated with ICG15. Finally, Nishie *et al*[2] demonstrated that Gd-EOB-DTPA-enhanced-MRI results of liver-to-spleen SI ratio and liver-to-major psoas muscle SI on the hepatobiliary phase were both well correlated with HH15 and LHL15. Thus, Gd-EOB-DTPA-enhanced MRI is expected to be useful for evaluating hepatic function in a similar way to the more widely used Tc-99m-GSA. In general, HH15 can reflect mild hepatic dysfunction and LHL15 can indicate severe hepatic dysfunction. In this study, Tc-99m-GSA indicated a strong correlation with

LHL15 for all patients except those with severe hepatic dysfunction according to the Child-Pugh classification. This seemingly incompatible finding might result from the fact that LHL15 reflects the accumulation of signal in the liver and thus has a stronger relationship with the rate of increase in hepatic signal. Furthermore, the Tc-99m-GSA parameters reflect the rate of increase in RI accumulation at 3 and 15 min. Therefore, the IR of the liver signal used in this study might be pharmacokinetically more similar to Tc-99m-GSA than LSC, because both IR and Tc-99m-GSA directly reflect uptake and excretion to hepatocytes. The uptake of Tc-99m-GSA in the liver may peak at 15 min after the infusion, and RI excretion from the hepatocytes could be ignored in the compartment model if it is only for 30 min. On the other hand, following the Gd-EOB-DTPA infusion, EOB was excreted in bile at an earlier stage than Tc-99m-GSA. Moreover, EOB is reportedly excreted in bile by 5 to 16 min after intravenous Gd-EOB-DTPA infusion in a normal liver[12], suggesting that EOB might be taken up by the cells 4 min after the infusion and the duration recorded might be the phase where the excretion to bile or blood flow was influenced less. In addition, in terms of the changes in liver SI over time after Gd-EOB-DTPA infusion, the signal increased 20 min after the infusion in the majority of subjects compared with that recorded 4 minutes after the infusion. However, it also decreased in 3 subjects, suggesting that the uptake of EOB into the liver might be lower according to the evaluation of this phase alone. EOB is secreted at least into the bile canaliculus and sinusoid. As for the cause of the excretion from hepatocytes, the excretory pathway could undergo changes in the presence of vascular lesions and / or biliary tract lesions and / or the rate of excretion to the sinusoid or bile canaliculus could vary among individuals. Both or either of these events could produce differences in the excretion of Gd-EOB-DTPA from the hepatic parenchyma, which is likely to influence the SI. It remains unclear from the data why the SI was decreased at 20 min in some patients ; however, it was assumed that in the 3 patients with signal decreases at 20 min the bile duct SI was increased because of accelerated excretion of Gd-EOB-DTPA from the liver cells, and these intensities varied widely. As far as we know, there are no reports on SIs in hepatic parenchyma or bile ducts, and further study is clearly needed.

This study result indicated that the correlation coefficient between the bilirubin level and ICG15 was slightly higher for the Tc-99m-GSA testing compared with 3T MRI using Gd-EOB-DTPA. Bilirubin is synthesized in the liver and released into the bile canaliculus, and in animal experiments conducted to evaluate excretory capacity by Kim *et al*[13], the relative SI value before imaging and the maximum and half maximum SI after imaging were all strongly correlated with the ICG15 and serum bilirubin level. ICG, bilirubin level, and Gd-EOB-DTPA have a common characteristic in that they are taken into the hepatic cells and excreted from them, which suggests that they may have similar intrahepatic kinetics. Furthermore, the relative value decreased in the patients with liver parenchymal injury caused by carbon tetrachloride, but did not decrease in the patients who underwent bile duct and /

or portal vein ligation, which suggested that posthepatic cholestasis might have less of an effect on the excretion of Gd-EOB-DTPA from hepatic cells. The study by Motosugi *et al*[1] demonstrated a strong negative correlation between the data of 20 min after EOB-MRI and ICG15, but no significant correlation with the serum bilirubin level.

The present study also found no correlation between IR_{20min} and serum bilirubin level, but a significant difference was observed with IR_{4min}, suggesting that the shorter time after infusion better reflected the excretory capacity of hepatic cells. Previous literature indicates that ICG15 showed the strongest correlation with some biochemical liver functional data[7,9], but this study could not reproduce these findings. Likewise, this study showed only a slight correlation with HH15 when Tc-99m-GSA was used. Factors underlying this contradiction might be the low number of subjects tested for ICG15, the small population (19 / 24 patients), and the accuracy of the test. However, no apparent cause could be found in the evaluable data and further studies are required. Unlike bilirubin, ICG enters hepatocytes via receptors according to individual hepatic function before being released into the bile canaliculus. Both these substances are excreted into the bile duct but are not released into the blood, suggesting that the kinetics were similar to those of Tc-99m-GSA.

Three cases in this study showed no complete visualization of contrast media inflow to the bile ducts at 20 min after the infusion. Takao *et al*[11] reported a peak SI in the bile ducts of normal liver at 30 min after infusion, while patients with hepatic dysfunction showed a peak delay and low SI. However, neither serological hepatic dysfunction nor any causes of stenosis, such as stones or tumors in the bile ducts, was observed in the present cases without complete visualization at 20 min after the infusion. The timing of bile excretion of Gd-EOB-DTPA varies among individuals, and was earlier than the peak time of the contrast effect in the bile ducts. Therefore, it was not clear whether the above-mentioned facts were directly reflected in the impaired bile excretion. The presence of mild cholangitis was suspected, although there were no effects on IR, HH15, or LHL15.

According to primary disease, the patients with hepatocellular carcinoma in this study might have had liver parenchymal injury caused by hepatitis and hepatic cirrhosis. The measurements were scattered, but the coefficient of correlation was slightly higher than that in the non-hepatocellular carcinoma group. Among the non-hepatocellular carcinoma group, the correlation between results of Gd-EOB-DTPA and Tc-99m-GSA was slightly lower in the cholangiocellular carcinoma group than in the hepatic metastases group. These findings suggested that the presence or absence of bile duct stenosis could affect excretion from the hepatic parenchyma, but the majority (87.5%) of cases in this study had contrast media inflow to the bile ducts 20 min after the infusion and this study could not elucidate whether liver parenchymal injury occurred. Finally, Kim *et al*[13] reported that bile duct stenosis is less likely to influence the excretion of Gd-EOB-DTPA. A larger study is required to elucidate these points.

A limitation of this study was that it was retrospective and in patients who were sched-

uled to undergo hepatectomy, thus there were relatively few participants and none of Grade C in the Child-Pugh classification. Nishie *et al*[2] reported good correlations in contrast ratio between the liver and iliopsoas with Tc-99m-GSA, and between the liver and spleen with LHL15 and HH15. Motosugi *et al*[1] also reported that there were significant correlations of the contrast ratios of liver and spleen with blood data. However, the present findings showed no significant correlations among LSC, Tc-99m-GSA, and blood data. Neither heterogeneity of the spleen parenchyma nor apparent stenosis in the splenic artery and vein was observed in this study, and so the cause for these differences in study results remains unknown. A larger prospective study should be performed in the future to clarify this issue, and to consider other timings after the infusion.

The costs to patients and the time needed for Tc-99m-GSA and Gd-EOB-MRI are approximately equal in Japan. Gd-EOB-MRI remains the standard test for hepatocellular carcinoma and hepatic metastases, and if the usefulness of Gd-EOB-MRI for assessing hepatic reserve is established, Tc-99m-GSA will no longer be used. However, Tc-99m-GSA was slightly better in the relationship with the liver function data in this study and methods for measuring Gd-EOB-MRI vary according to the literature. Therefore, a standard method of assessing hepatic reserve using Gd-EOB-MRI should be established like those used for Tc-99m-GSA. Currently, Tc-99m-GSA should be the first choice ; however, in the case of applying Gd-EOB-MRI alone, the method used in this study will be worthwhile in the clinical setting.

Furthermore, the results suggested that Gd-EOB-DTPA-enhanced MRI could be used to assess hepatic reserve by determining the increase in liver signal similar to Tc-99m-GSA.

Conclusion

There were significant correlations between the IR of the liver signal and the LSC as shown by Gd-EOB-DTPA-enhanced MRI, and between HH15 and LHL15 as demonstrated by Tc-99m-GSA scintigraphy. The highest coefficient of correlation was obtained with the IR at 4 min, suggesting that IR of the liver signal measured by Gd-EOB-DTPA-enhanced MRI might be a useful parameter for evaluating hepatic function.

References

1) Motosugi U, Ichikawa T, Sou H, Sano K, Tominaga L, Kitamura T and Araki T : Liver parenchymal enhancement of hepatocyte-phase images in Gd-EOB-DTPA-enhanced MR imaging : which biological markers of the liver function affect the enhancement? *J Magn Reson Imaging* **30** : 1042–1046 (2009)

2) Nishie A, Ushijima Y, Tajima T, Asayama Y, Ishigami K, Kakihara D, Nakayama T, Takayama Y, Okamoto D, Abe K, Obara M, Yoshimitsu K and Honda H : Quantitative analysis of liver function using superparamagnetic iron oxide- and Gd-EOB-DTPA-enhanced MRI : comparison with Technetium-99m galactosyl serum albumin scintigraphy. *Eur J Radiol* **81** : 1100–1104 (2011)

3) Tschirch FT, Struwe A, Petrowsky H, Kakales I, Marincek B and Weishaupt D : Contrast-enhanced MR cholangiography with Gd-EOB-DTPA in patients with liver cirrhosis : visualization of the biliary ducts in comparison

with patients with normal liver parenchyma. *Eur Radiol* **18**：1577-1586（2008）
4) Ryeom HK, Kim SH, Kim JY, Kim HJ, Lee JM, Chang YM, Kim YS and Kang DS: Quantitative evaluation of liver function with MRI Using Gd-EOB-DTPA. *Korean J Radiol* **5**：231-239（2004）
5) Nilsson H, Nordell A, Vargas R, Douglas L, Jonas E and Blomqvist L: Assessment of hepatic extraction fraction and input relative blood flow using dynamic hepatocyte-specific contrast-enhanced MRI. *J Magn Reson Imaging* **29**：1323-1331（2009）
6) Torizuka K, Ha-Kawa SK, Kudo M, Kubota Y, Yamamoto K, Itoh K, Nagao K, Uchiyama G, Koizumi K, Sasaki Y, Kosaka N, Murata H, Murashima N, Kosuda S, Suzuki K, Ishii K, Ishii K, Imaeda T, Kanematsu M, Nakamura K, Nakagawa T, Hisada K, Aburano T, Nakajima T, Ishii Y, Morita R, Suzuki T, Kubo S, Konishi J, Ohishi H, Imai T, Tanaka Y, Kitagawa S, Inoue K, Kashiwagi T, Kozuka T, Shiomi S, Ochi H, Hasegawa Y, Sasaki Y, Ikekubo K, Hino M, Niiya H, Hiraki Y, Tanabe M, Kawasaki Y, Tsuda T, Hamamoto K, Masuda K, and Ichiya Y: Phase III multi-center clinical study on 99mTc-GSA, a new agent for functional imaging of the liver. *Kaku Igaku* **29**：159-181（1992）（in Japanese）
7) Kubota Y, Kitagawa S, Inoue K, Ha-Kawa SK, Kojima M and Tanaka Y: Hepatic functional scintigraphic imaging with 99mtechnetium galactosyl serum albumin. *Hepatogastroenterology* **40**：32-36（1993）
8) Satoh K, Yamamoto Y, Nishiyama Y, Wakabayashi H and Ohkawa M: 99mTc-GSA liver dynamic SPECT for the preoperative assessment of hepatectomy. *Ann Nucl Med* **17**：61-67（2003）
9) Iida T, Isaji S, Yagi S, Hori T, Taniguchi K, Ohsawa I, Mizuno S, Usui M, Sakurai H, Yamagiwa K, Yamakado K and Uemoto S: Assessment of liver graft function and regeneration by galactosyl-human serum albumin（99mTc-GSA）liver scintigraphy in adult living-donor liver transplantation. *Clin Transplant* **23**：271-277（2009）
10) Kaibori M, Ha-Kawa SK, Uchida Y, Ishizaki M, Saito T, Matsui K, Hirohara J, Tanaka K and Kamiyama Y: Liver regeneration in donors evaluated by Tc-99m-GSA scintigraphy after living donor liver transplantation. *Dig Dis Sci* **53**：850-855（2008）
11) Takao H, Akai H, Tajima T, Kiryu S, Watanabe Y, Imamura H, Akahane M, Yoshioka N, Kokudo N and Ohtomo K: MR imaging of the biliary tract with Gd-EOB-DTPA: effect of liver function on signal intensity. *Eur J Radiol* **77**：325-329（2011）
12) Bollow M, Taupitz M, Hamm B, Staks T, Wolf KJ and Weinmann HJ: Gadolinium-ethoxybenzyl-DTPA as a hepatobiliary contrast agent for use in MRI cholangiography: results of an in vivo phase-I clinical evaluation. *Eur Radiol* **7**：126-132（1997）
13) Kim T, Murakami T, Hasuike Y, Gotoh M, Kato N, Takahashi M, Miyazawa T, Narumi Y, Monden M and Nakamura H: Experimental hepatic dysfunction: evaluation by MRI with Gd-EOB-DTPA. *J Magn Reson Imaging* **7**：683-688（1997）

［Received December 1, 2011: Accepted February 1, 2012］